Decrease in β-Cell Mass Leads to Impaired Pulsatile Insulin Secretion, Reduced Postprandial Hepatic Insulin Clearance, and Relative Hyperglucagonemia in the Minipig

Lise L. Kjems,[1] Barbara M. Kirby,[1] Elizabeth M. Welsh,[1] Johannes D. Veldhuis,[2] Marty Straume,[2] Susan S. McIntyre,[1] Dongchang Yang,[1] Pierre Lefèbvre,[3] and Peter C. Butler[1]

Most insulin is secreted in discrete pulses at an interval of ~6 min. Increased insulin secretion after meal ingestion is achieved through the mechanism of amplification of the burst mass. Conversely, in type 2 diabetes, insulin secretion is impaired as a consequence of decreased insulin pulse mass. β-cell mass is reported to be deficient in type 2 diabetes. We tested the hypothesis that decreased β-cell mass leads to decreased insulin pulse mass. Insulin secretion was examined before and after an ~60% decrease in β-cell mass achieved by a single injection of alloxan in a porcine model. Alloxan injection resulted in stable diabetes (fasting plasma glucose 7.4 ± 1.1 vs. 4.4 ± 0.1 mmol/l; $P < 0.01$) with impaired insulin secretion in the fasting and fed states and during a hyperglycemic clamp (decreased by 54, 80, and 90%, respectively). Deconvolution analysis revealed a selective decrease in insulin pulse mass (by 54, 60, and 90%) with no change in pulse frequency. Rhythm analysis revealed no change in the periodicity of regular oscillations after alloxan administration in the fasting state but was unable to detect stable rhythms reliably after enteric or intravenous glucose stimulation. After alloxan administration, insulin secretion and insulin pulse mass (but not insulin pulse interval) decreased in relation to β-cell mass. However, the decreased pulse mass (and pulse amplitude delivered to the liver) was associated with a decrease in hepatic insulin clearance, which partially offset the decreased insulin secretion. Despite hyperglycemia, postprandial glucagon concentrations were increased after alloxan administration (103.4 ± 6.3 vs. 92.2 ± 2.5 pg/ml; $P < 0.01$). We conclude that an alloxan-induced selective decrease in β-cell mass leads to deficient insulin secretion by attenuating insulin pulse mass, and that the latter is associated with decreased hepatic insulin clearance and relative hyperglucagonemia, thereby emulating the pattern of islet dysfunction observed in type 2 diabetes. *Diabetes* 50: 2001–2012, 2001

Type 2 diabetes is characterized by impaired glucose-mediated insulin secretion (1,2). This has been documented by demonstrating reduced first-phase insulin release in response to intravenous glucose (3,4) and impaired insulin release after glucose ingestion (1,5) and during a hyperglycemic clamp (6). Further analyses indicate that most insulin secretion is derived from discrete insulin secretory bursts (7,8), the mass of which is diminished in patients with type 2 diabetes (9). In addition, it has been reported that β-cell mass may be decreased in patients with type 2 diabetes (10), although this remains controversial. Indeed, the role of any decrease in the β-cell mass in the pathogenesis of impaired insulin secretion and the pathogenesis of hyperglycemia in type 2 diabetes remains uncertain.

In the present study, we addressed the hypothesis that defective insulin secretion in type 2 diabetes can be recapitulated by a selective decrease in β-cell mass. To test this postulate, we examined the pattern of insulin secretion in a porcine minipig model before and after induction of partial selective β-cell loss by use of alloxan. The extent of the decrement in β-cell mass was measured by morphometric analysis. Specifically, we examined insulin release in response to a mixed meal to reproduce conditions of daily living as well as in response to a hyperglycemic clamp and an acute intravenous glucose bolus. We therefore tested the hypothesis that a selective decrease in β-cell mass induces an impaired glucose-stimulated insulin secretion and insulin pulse mass and that these changes are related to β-cell mass.

RESEARCH DESIGN AND METHODS

Study design. The study was designed to examine the effect of a decrease in β-cell mass on the pattern of insulin secretion. First, we established the parameters for pulsatile insulin detection in the pig (protocol 1). Second, we investigated the effects of a decreased β-cell mass achieved by a pharmacological dose of alloxan on pulsatile insulin secretion. The dynamics of insulin secretion were studied in response to a mixed meal (protocol 2) and during a hyperglycemic clamp (protocol 3). Two animals (one male and one female) completed protocol 1, seven animals (five males and two females) completed protocol 2, and 5 animals completed protocol 3. Finally, we measured β-cell mass in the pigs included in the studies. In addition, four pigs started protocol 2 or 3 but did not complete them, as sampling catheters were lost. When

From the [1]Diabetes Research Unit and Royal (Dick) School of Veterinary Studies, University of Edinburgh, Edinburgh, Scotland; [2]Center for Biological Timing and Division of Endocrinology and Metabolism, University of Virginia, Charlottesville, Virginia; and [3]Division of Diabetes, Nutrition and Metabolic Disorders, Department of Medicine, University of Liege, Liege, Belgium.

Address correspondence and reprint requests to Dr. Peter C. Butler, Division of Endocrinology and Diabetes, Keck School of Medicine, University of Southern California, 1333 San Pablo Street, BMT-B11, Los Angeles, CA 90033. E-mail: pbutler@hsc.usc.edu.

Received for publication 15 September 2000 and accepted in revised form 16 May 2001.

P.C.B. received an unrestricted grant from Novo Nordisk to assist in the development of the porcine model used in this study.

ELISA, enzyme-linked immunosorbent assay.

available, the data obtained from these pigs was included in the correlations shown in Figs. 2 and 9.

Preparation of animals for study. All studies were approved by the Scottish Home Office (equivalent to the Animal Use and Care Committee in the U.S.). A total of 12 Gottingen minipigs (11) (9 males and 3 females) that were 1–3 years old and weighed 20–32 kg were studied. The animals were obtained from Ellegaards Gottingen Minipigs (Gottingen, Denmark), where they were kept in a barrier unit for the first year. In Edinburgh, the pigs were housed under controlled conditions, 12-h light/12-h dark, fed twice daily a total of 450 g of Minipigs Maintenance Diet (9.28 MJ/kg; SDS, Edinburgh, U.K.), 13.8% protein, 51.2% nitrogen-free extract (equivalent to carbohydrate content), 2.5% fat, 12.7% fiber, and 12% water and allowed free access to water. Body temperature, hematocrit, and weight were recorded once a week, and the animals were exercised on a daily basis. The pigs were studied at least 10 days after surgery when they were eating normally, had normal stools, were maintaining weight, and had normal hemoglobin and leukocyte count and normal renal and liver function. Before the study, all pigs were acclimatized to the laboratory and staff.

The technique of surgical implantation of the portal vein sampling catheter (protocol 1 only), arterial catheters, and jugular venous catheters (protocols 1, 2, and 3) was adapted from a canine model described previously (7). In brief, with the pigs under general anesthesia, the portal vein was isolated for a distance of 3–4 cm cranial to the pancreaticoduodenal venous tributary, and a catheter was inserted and advanced cephalic until its tip was located at the bifurcation of the portal vein. A catheter was implanted similarly in the splenic vein, and both catheters exited the left flank and tunneled to the intrascapular area.

The left jugular vein and carotid artery were exposed by cut-down and were catheterized, and the free ends of the catheters tunneled to the left dorsal interscapular area. The catheters were filled carefully to capacity with heparin (10,000 IU/ml) and color-labeled for later identification. The catheters were protected by a vest. Ampicillin (20 mg/kg; SmithKline Beecham, Dublin, Ireland) was given intravenously pre- and postoperatively for infection prophylaxis. Buprenorphine 0.01 mg/kg was given by epidural infusion after induction of anesthesia as analgesic cover for 24 h. This was supplemented by a bolus of Zenecarp 4 mg/kg (Parke Davis, Eastleigh, U.K.) administered intravenously at the end of the surgical procedure. A mix of buprenorphine (0.01 mg/kg) and Zenecarp (2 mg/kg) was given intravenously twice daily postoperatively until the animal had recovered fully from the procedure. Body temperature was measured daily for 7 days postoperatively, and antibiotics were administered only when there were signs of postoperative infection. Patency of catheters was checked every day. The catheter exteriorization site was cleaned regularly with hydrogen peroxide (4%), and Bactroban cream (SmithKline Beecham) was applied.

Reduction of β-cell mass with alloxan. β-cell mass was reduced by intravenous injection of alloxan monohydrate (Sigma, Dorset, U.K.). The alloxan was refrigerated in a dessicator until used; all alloxan doses were made up from the same batch. The alloxan was weighed out immediately before administration in a 0.1N acetic acid solution (Sigma, Dorset, U.K.), pH 4.4. A dose of 80 mg/kg was diluted in the buffer to a volume of 1.2 ml stock solution/kg. Immediately after preparation, the solution was injected as a bolus through a 0.22-μm Millipore filter (Sigma, Dorset, U.K.) into the jugular vein over 1 min, immediately after which the animals were fed. All of the animals developed mild to moderate hyperglycemia (range 6–11 mmol/l) within the first 24 h after alloxan administration, but this was not treated with insulin until 48 h after alloxan administration. After 48 h, the animals were treated only with insulin (Velosulin, Novo Nordisk A/S, Bagsvaerd, Denmark) if the fasting plasma glucose was above 9 mmol/l (n = 1/7) or if the animal had glucosuria (n = 1/7, the same animal). Plasma glucose was measured daily and urinalysis was performed (Chemstrip, Boehringer Mannheim, U.K.) twice a week to check for glucose, ketones, pH, and protein. No pig developed ketonuria. The diabetic animal that received insulin had no insulin on the morning of the experiments.

Postmortem. Pancreata were retrieved at the end of the 8-week experimental series. The animals were killed with phenobarbital, and after exposure through a midline incision, the gastrointestinal block was removed in toto including the pancreatic tissue surrounding the caudal vena cava inferior and kept in ice-cold saline. The volume and the weight of the pancreas were determined, and the tissue then was dissected immediately on a cold cutting board and kept on ice to prevent autodigestion. Sequential 1-cm samples were fixed in 10% neutral-buffered formaldehyde and then embedded in paraffin. Sections from each block subsequently were immunostained for insulin (guinea pig anti-porcine, 1:1,000; Dako, Carpinteria, CA).

Assays. Insulin concentrations in plasma samples were measured in duplicate by an enzyme-linked immunosorbent assay (ELISA) (12) modified for porcine insulin. The assay is based on two monoclonal murine antibodies specific for intact human insulin. The operating range is from 5 to 2,000 pmol/l, recovery 85–120%, and the assay is linear up to 2,000 pmol/l. Glucagon samples were measured by radioimmunoassay as described previously (13). Glucose was measured by the glucose oxidase technique using a Beckman Glucose Analyser (Fullerton, CA).

Study protocols

Protocol 1a: insulin kinetics. Deconvolution of insulin secretion from plasma insulin concentration profiles requires knowledge of the decay characteristics (i.e., mono vs. biexponential decay values) in the sampling pool of interest. We established these measures by administration of a bolus of 80 mU of human insulin injected over 30 s via a catheter implanted in the splenic vein while endogenous insulin secretion was suppressed by a somatostatin infusion (Bachem Ltd., Essex, U.K.) 0.1 $\mu g \cdot kg^{-1} \cdot min^{-1}$. Insulin (Actrapid, Novo Nordisk A/S) was dissolved in saline and 0.25% porcine albumin (a gift of Novo Nordisk). After the insulin bolus, blood was sampled from both the portal vein and the carotid artery catheters at 15-s intervals for 5 min, every minute for the next 20 min, and every 5 min for the next 25 min. At time 60 min, a constant insulin infusion (1 $mU \cdot kg^{-1} \cdot min^{-1}$, Actrapid) was given via the same splenic vein catheter and continued for 65 min (to t = 125 min). At time 120 min, blood was sampled at 15-s intervals for 5 min, then every min for 15 min until 140 min, and thereafter every 5 min until 220 min (all samples collected simultaneously from the portal vein catheter and the artery). Throughout this protocol, blood glucose was measured every 5 min and a variable glucose infusion was given to maintain euglycemia.

Protocol 1b: portal versus systemic sampling for measurement of pulsatile insulin secretion. Although the portal sampling site (versus the systemic circulation) enhances the detection of insulin pulses, it requires invasive intra-abdominal surgery to implant portal vein catheters. We recently reported in humans that use of a highly specific two-site ELISA insulin assay allows accurate detection of insulin pulses sampled from the systemic circulation (14). The purpose of protocol 1b was to extend this observation to the pig to verify use of a systemic sampling site for pulse detection. Portal vein and arterial catheters were implanted in two pigs. Blood was sampled at 1-min intervals simultaneously from the arterial and portal vein catheters in basal (fasting) conditions and during a hyperglycemic clamp (glucose 9 mmol/l) and after a mixed meal (hyperglycemic clamp and meal methods described below in protocols 2 and 3). These data were examined subsequently by deconvolution using criteria for portal versus arterial sampling obtained in protocol 1a.

Protocol 2: mixed meal. Pigs (n = 7) were trained to eat a mixed meal that contained glucose in sugar-free jelly (U.S. equivalent Jell-O) mixed with Minipig Maintenance Diet. After a 16-h fast, pigs were placed in a restraining box and the sampling catheters were aspirated and flushed in preparation for sampling. A blood sample was obtained from the artery to determine the hematocrit. Saline 0.9% was infused via the jugular vein catheter at 30 ml/h throughout the study (from t = −40 to 210 min). At t = 0 min, a mixed meal consisting of 2.2 g/kg D-glucose in sugar-free jelly mixed with 50 g of Minipig Maintenance Diet was provided. Blood samples (1.0 ml) were obtained from an arterial catheter (n = 5) at 1-min intervals from −40 to 90 min, every 5 min from 90 to 160 min, and then every 10 min until 210 min for measurement of plasma insulin. Arterial blood samples also were obtained at 5-min intervals from −40 to 160 min and at 10-min intervals from 160 to 210 min for measurement of plasma glucose concentrations. Arterial blood samples were collected for measurement of plasma glucagon concentration at 30-min intervals throughout the study (−40 to 10).

The samples for insulin were drawn into chilled polyethylene tubes that contained EDTA, placed on ice, and centrifuged within 5 min of collection (2 min, 15,000 rpm). Plasma was separated into two tubes and frozen at −20°C for later analysis. The blood glucose samples were drawn into tubes that contained heparin and sodium fluoride, centrifuged, and measured immediately by the glucose oxidase technique (Beckman).

Protocol 3: hyperglycemic clamp. Pigs (n = 5) were prepared as in protocol 1. From −40 to 0 min, insulin secretion was evaluated in the fasting state at the prevailing fasting glucose concentration. From t = 0 to t = 70, the plasma glucose was increased to 8 mmol/l by a glucose infusion. Insulin secretion then was evaluated at steady-state hyperglycemia from t = 30 to t = 70 min. First-phase insulin secretion was evaluated in response to an intravenous glucose bolus (0.3 g/kg) given at t = 70 min. Blood samples (1.0 ml) for subsequent insulin assay were taken from the arterial catheter at 1-min intervals from t = −40 to t = 0 min and from t = 30 to t = 90 min. Blood samples for subsequent glucose measurement were taken every 5 min from the arterial catheter from t = 30 to t = 90 min.

Calculations.

Protocol 1a: insulin kinetics. Analysis of the insulin disappearance profiles best fit a single (arterial) or two-component (portal) exponential model, respectively. The biexponential decay observed at the portal vein is consistent with other regional sampling catheters proximate to the site of the secretory

burst; the first decay component presumably reflected mixing of hormone within the regional venous blood and its movement through the regional sampling site by blood flow. The rate constant was obtained by interactive curve fitting. The parameters were estimated by Gauss-Newton iteration with confidence intervals for the precision of fit defined by Monte Carlo exploration of the joint parameter spaces.

Protocol 1b: portal versus arterial sampling routes for pulse detection. A comparison of the corresponding arterial versus portal vein plasma insulin concentration profiles was made by inspection as well as cross-correlation analyses of pulse location and magnitude observed in the corresponding deconvolved insulin secretion profiles.

Protocols 2 and 3: glucose, insulin, and glucagon concentration data. The mean fasting plasma glucose, insulin, and glucagon concentration was calculated in each pig before and after alloxan administration. The mean concentration (and/or area under the concentration curve by the trapezoidal rule) of each of these parameters also was measured during the clamp and after meal ingestion. The glucose/insulin concentration ratio was calculated in each pig 30 min after meal ingestion. The first-phase insulin response to glucose bolus injection was quantified by calculating the area under the curve of the plasma insulin concentration profile by the trapezoidal rule during the 12 min after glucose injection at the end of the hyperglycemic clamp. Pulsatile insulin secretion was quantified by use of a deconvolution method developed by Veldhuis and Johnson (15) and was specifically validated for this purpose in a canine model (7). In brief, the 1-min plasma (duplicate) insulin concentration time series were deconvolved by a multiparameter technique with the following assumptions. The arterial plasma insulin concentration in each animal, as monitored at frequent intervals, results from five determinable and correlated parameters: *1*) a finite number of discrete insulin secretory bursts occurring at specific times and having *2*) individual amplitudes (maximal rate of insulin secretion within a burst), *3*) a common half-duration (duration of an algebraically Gaussian secretory profile), superimposed on a *4*) basal time invariant insulin secretory rate, and *5*) a monoexponential insulin disappearance model in the systemic circulation. The last parameter consisted of an estimated half-life of 2.8 min and a slow fractional compartment of 0.065 as measured directly with the same assays. Assuming the forgoing nominal insulin disappearance values, we estimated the numbers, locations, amplitudes, and half-duration of insulin secretory bursts, as well as a nonnegative basal insulin secretory rate for each data set using nonlinear least square fitting of the multiparameter convolution for each insulin time series. A modified Gauss-Newton quadratically convergent iterative technique was used with an inverse (sample variance) weighting function. Parameters were estimated until their predicted values and the total fitted variance both varied by <1 part in 100,000. Asymmetric, highly correlated joint variance spaces were calculated for each parameter by the Monte Carlo support plane procedure. Secretory rates are expressed as mass units of insulin (picomoles) released per unit of distribution volume (liters) per unit of time (minutes). The mass of hormone secreted per burst (time integral of the calculated secretory burst) thus is computed as picomoles of insulin released per liter of volume of distribution. The percentage of insulin delivered into the circulation in discrete insulin bursts was calculated as described previously (7).

Evidence of regular periodicity (oscillations) in insulin concentration was examined by two independent techniques, CORRCOS (16) and Fast Fourier Transform-Nonlinear Least Squares (17). Because they led to the same conclusion, we report the data obtained by CORRCOS only. CORRCOS is a fully automated analytical algorithm for quantitative detection and statistical characterization of rhythmic changes in a time series measurement of the feature of interest (here insulin concentration) (16).

The pseudo steady-state clearance rate of endogenously secreted insulin was calculated by the equation C (l/min) = S (pmol/min)/I (pmol/l), where C = insulin clearance rate, S = insulin secretion rate (quantified by deconvolution), and I = arterial plasma insulin concentration.

β-cell mass. Pancreatic sections immunostained for insulin were evaluated to determine the percentage of pancreatic cross-sectional area that was positive for β-cells. Islets clearly were present in all slides. An average of 482 islets (range 181–777) were included in evaluations of each pig. The β-cell mass then was calculated by the product of the β-cell fraction of pancreas cross-sectional area and the pancreatic weight. Because pigs served as their own controls (studied before and after alloxan administration), it was not possible to determine β-cell mass before alloxan administration in the seven pigs that underwent protocols 2 and 3. Therefore, correlations of β-cell mass focused on β-cell mass after alloxan administration versus parameters of insulin secretion. Three pigs that did not receive alloxan (used in protocol 1) were available; therefore, these three pigs provided an estimate of normal β-cell mass in this minipig model and an estimate of percentage decrease in β-cell mass after alloxan administration in study pigs. In conclusion, pancreas was obtained from three pigs that did not receive alloxan and from seven pigs that did receive alloxan.

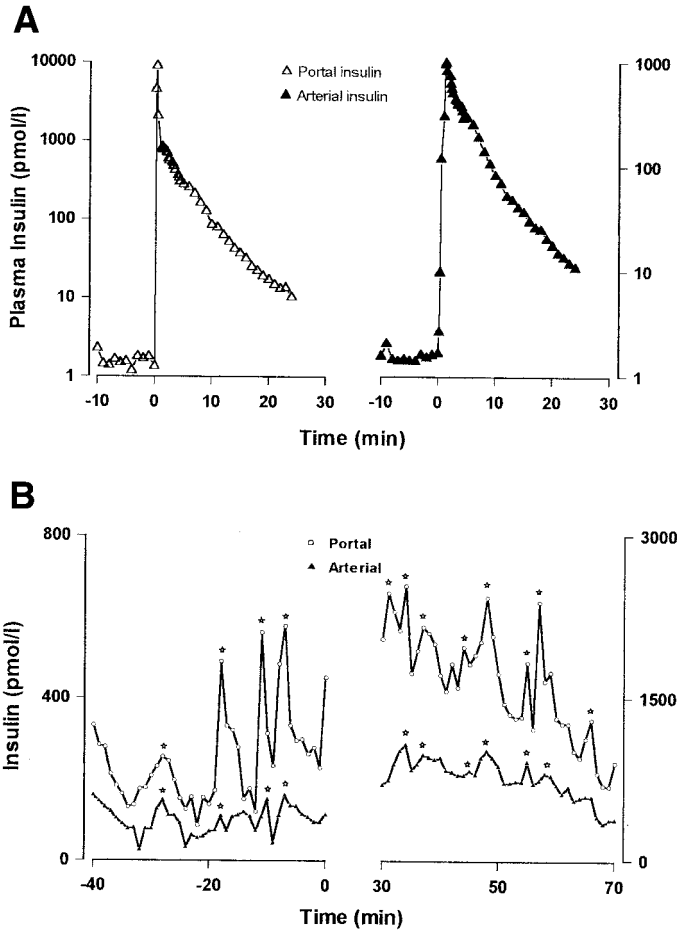

FIG. 1. *A*: The plasma insulin concentrations in minipigs at the portal and arterial sampling site after a bolus of insulin (80 mU) was injected into the splenic vein at $t = 0$ min during a somatostatin infusion to inhibit endogenous insulin secretion. The decay curve of the log insulin concentration was monoexponential at the arterial and biexponential at the portal sampling site. *B*: Simultaneous plasma insulin concentrations in the portal vein and the arterial sampling sites in the fasting state (−40 to 0 min) and during a hyperglycemic clamp (30–70 min) in a representative pig. The presence of a detected pulse is shown by a star. There is a close relationship between the pulses detected in the portal and arterial sampling sites.

Statistical analysis. Data are presented as the mean and standard error of the mean. The impact of alloxan treatment on the stated parameters of insulin secretion was determined by using the two-tailed paired Student's t test. Regression analysis was used to determine the relationship between variables. $P < 0.05$ was taken as evidence of statistical significance.

RESULTS

Protocol 1: parameters for detection of pulsatile insulin secretion.

Protocol 1a: insulin kinetics. The plasma insulin concentration decay curves in the portal vein and the carotid artery after a bolus injection into a superior mesenteric vein are shown in Fig. 1*A*. The observed insulin concentration decay curve was monoexponential when sampling from the systemic circulation and biexponential when sampling from the portal vein. After discontinuation of the constant insulin infusion, the portal vein decay curve was monoexponential, the slope corresponding to the second component observed from the same sampling site after a bolus injection. The slow-phase half-life obtained from the

TABLE 1
Demographic data

	Before alloxan	After alloxan
Age (months)	20.8 ± 4.2	
Sex (M/F)	5/2	
Weight (kg)	25.2 ± 1.9	24.5 ± 1.8
Glucose (mmol/l)	4.4 ± 0.1	7.4 ± 1.1*
Insulin (pmol/l)	86.0 ± 17.3	55 ± 7.5*
Glucagon (pg/ml)	110 ± 16	105 ± 4.1

Data are means ± SD or n. The age, sex, weight, and fasting plasma glucose, insulin, and glucagon concentrations in pigs included in protocol 2 ($n = 7$) before and after alloxan administration (*$P <$ 0.05). Five of these pigs were used in protocol 3.

portal vein sampling site therefore was calculated from the decay curve after constant insulin infusion, which was 2.8 min. This was used to calculate the first half-life after bolus injection, which equalled 0.8 min with a slow fractional component of 0.65. The calculated half-life for insulin in the systemic circulation was calculated both from the decay data after discontinuation of the constant insulin infusion (3.0 min) and from the decay data after the bolus insulin injection (2.8 min). The calculated effective volume of distribution for insulin after bolus injection into the splenic vein with sampling from the arterial catheter was 163 ml/kg body wt.

Protocol 1b: portal versus arterial sampling sites. In both the fasting and the stimulated (meal or hyperglycemic clamp) states, distinct pulses in the concentration of insulin were apparent in both the arterial and the portal vein profiles. Figure 1*B* illustrates that pulses of insulin detected in the portal circulation (signified by the stars) correspond well to those detected in the arterial circulation in the conditions of the present studies, although as expected, the amplitude of these pulses is greater in portal vein.

Protocol 2: responses to meal ingestion.

Body weight, β-cell mass, and diabetic status. Body weight and hepatic and renal biochemical parameters were unchanged after alloxan administration. As expected, administration of alloxan ($n = 7$ animals) resulted in a spectrum of changes in carbohydrate metabolism in individual pigs, ranging from glucose intolerance ($n = 4$) to diabetes ($n = 3$). The mean β-cell mass in the seven pigs that received alloxan was 41.5 ± 14.1% of that in control pigs and varied from 5.6 to 133% (Table 1; Fig. 2).

Glucose, insulin, and glucagon concentrations. After alloxan administration, the mean fasting plasma glucose concentration ($t = -40$ to 0 min) was increased (7.7 ± 0.1 vs. 4.5 ± 0.1; $P < 0.05$) and increased further after meal ingestion (glucose concentration at 20 min 9.9 ± 1.4 vs. 6.3 ± 0.61 mmol/l; $P < 0.02$). Alloxan led to a modest decrease in the fasting plasma insulin concentration (55 ± 7.5 vs. 86 ± 17.3 pmol/l; $P < 0.01$). After the mixed meal, despite marked hyperglycemia, the rise in plasma insulin concentration was suppressed (insulin concentration at 20 min 276.4 ± 85.8 vs. 479.9 ± 125.6 pmol/l; $P < 0.05$), confirming the presence of a marked defect in meal-stimulated insulin secretion. Thirty minutes after meal ingestion, the glucose/insulin concentration ratio ([mmol/l × 10]/pmol) was markedly increased in pigs after alloxan treatment ($P < 0.01$). Alloxan treatment did not alter fasting plasma glucagon concentrations, which, given the corresponding hyperglycemia, suggests impaired suppression of glucagon secretion. However, after ingestion of the mixed meal, despite marked hyperglycemia after alloxan administration, the plasma glucagon concentration was increased compared with before alloxan administration (postprandial glucagon concentration 103 ± 6.3 vs. 92 ± 2.5 pg/ml; $P < 0.01$), emphasizing the failure of the α-cells to suppress glucagon release in response to hyperglycemia (Figs. 2 and 3).

Total and pulsatile insulin secretion. Examination of the insulin concentration profiles before and after meal ingestion and alloxan administration (Fig. 4) indicated that the increased insulin secretion after a meal was accompanied normally by a marked increase in the amplitude of the insulin concentration pulses and that the extent of this increase was attenuated after alloxan administration. The calculated insulin secretion rate (Fig. 5) revealed deficient insulin secretion in the fasting state (~50% reduction) and strikingly so after meal ingestion (~80% reduction) after alloxan treatment. The posthepatic percentage of insulin

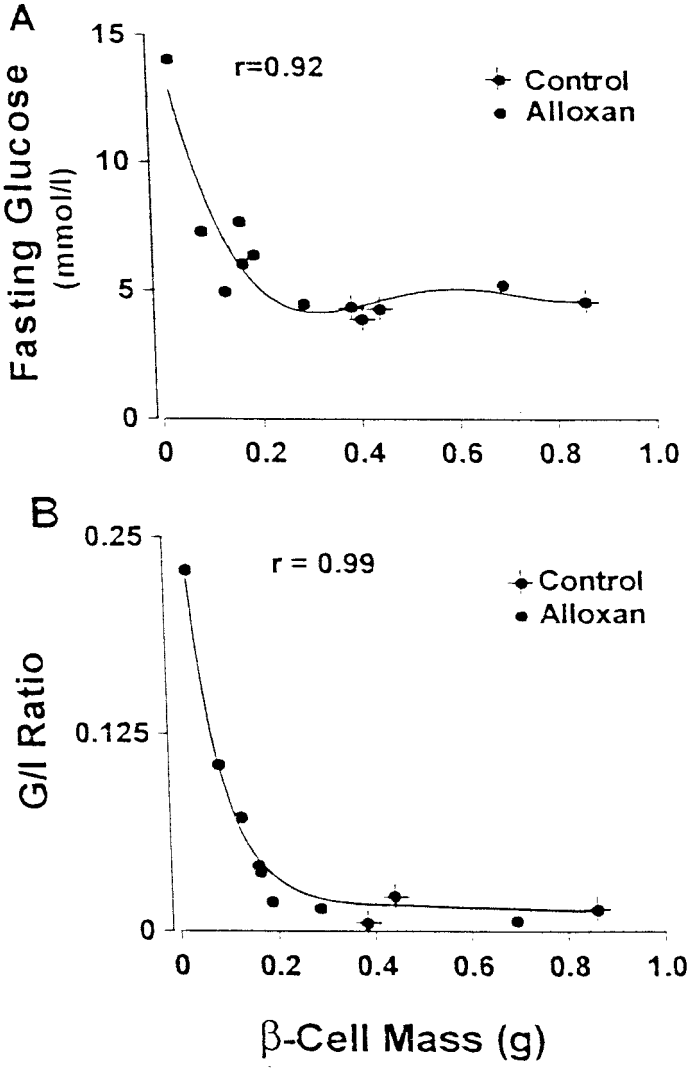

FIG. 2. The relationship between the β-cell mass and the fasting plasma glucose concentrations (*A*) and the plasma glucose/insulin concentration ratio ([mmol/l × 10]/pmol/l) 30 min after the meal (*B*) in pigs that had been treated with alloxan ($n = 8$) and pigs that had not received alloxan ($n = 4$ in *A*; $n = 3$ in *B*).

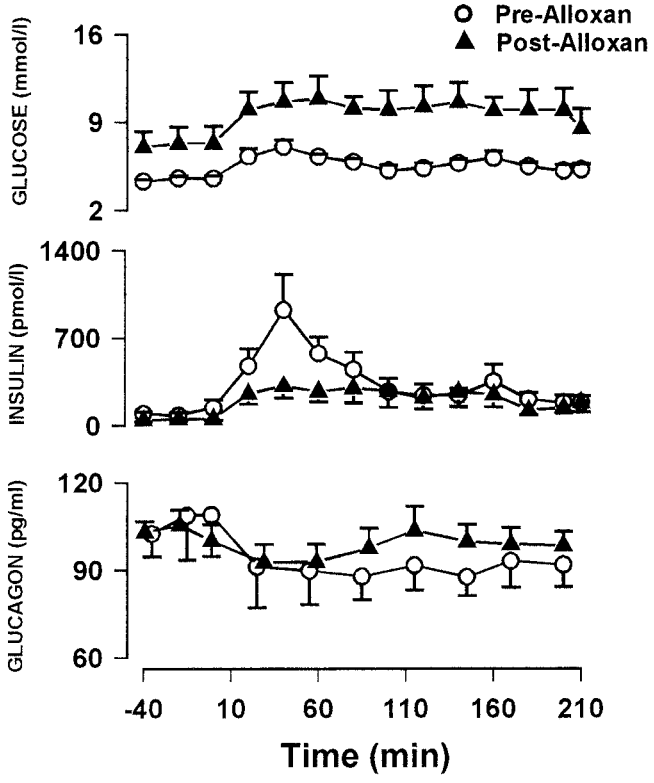

FIG. 3. The mean plasma glucose (top), insulin (middle), and glucagon (bottom) concentrations before (−40 to 0 min) and after (0–210 min) ingestion of a mixed meal.

derived from discrete insulin secretory bursts (~60%) was unaffected by alloxan treatment and comparable to that reported previously when also measured by sampling from the systemic circulation (18). When the insulin concentration profiles were subjected to deconvolution analysis (Figs. 5 and 6), we observed a selective decrease in insulin burst mass (decreased by 54% in the fasting state and 63% after meal ingestion after alloxan administration). In contrast, there was no change in the frequency of pulsatile insulin secretion (Table 2).

When the insulin concentration data were examined for regular periodicity by CORRCOS, statistically significant regular oscillations were detected in five of the seven pigs in the fasting state both before and after alloxan administration but in only two of the seven pigs after meal ingestion. In the five pigs with oscillations present in the fasting state, the oscillation interval was unchanged before versus after alloxan administration (12.3 ± 1.7 vs. 12.9 ± 1.2 min).

Insulin clearance. The calculated insulin clearance rate (Fig. 7) for endogenously secreted insulin was slightly lower in the fasting state ($P < 0.05$) after alloxan administration. However, previous alloxan treatment lead to an ~40% decline in insulin clearance rate after meal ingestion ($P < 0.01$). The insulin clearance rate was correlated with the amplitude of insulin pulse mass ($r = 0.62$, $P < 0.001$; Fig. 8).

Relationship of insulin secretion to β-cell mass. Pigs that had been treated with alloxan after meal ingestion showed a strong positive correlation among the insulin secretion rate ($r = 0.98$, $P < 0.01$), the insulin pulse mass ($r = 0.98$, $P < 0.001$), and the 30-min postprandial insulin concentration ($r = 0.6$, $P < 0.001$) and the β-cell mass. However, there was no relationship between β-cell mass and insulin pulse interval ($r = -0.14$, P = NS). Inspection of the relationship between the fasting plasma glucose concentration or the 30-min postprandial glucose/insulin ratio versus the β-cell mass (Fig. 2) is instructive. These data suggest that there is a fairly wide range of β-cell mass that will suffice to accomplish glucose homeostasis. They also suggest that if the β-cell mass is decreased beyond a critical level (~0.2 g in this porcine model), then there is insufficient insulin to retain glucose homeostasis, particularly in the fed state (Fig. 9).

Protocol 3: hyperglycemic clamp.

Glucose and insulin concentration and glucose infusion rates. Before the clamp, the patterns of the plasma glucose and insulin concentrations corresponded to those observed before meal ingestion in protocol 2. During the clamp, the glucose concentrations were comparable before and after alloxan administration (8.4 ± 0.5 vs. 9.8 ± 0.8 mmol/l). The glucose infusion rate required to achieve this (protocol time 30–70 min) was greater before versus after alloxan administration (12.5 ± 0.3 vs. 1.6 ± 0.7 mg · kg^{-1} · min^{-1}; $P < 0.01$). Despite the comparable glucose concentrations during the clamp, the plasma insulin concentration was decreased after alloxan administration, suggesting a defect in insulin secretion (Fig. 10; Table 2).

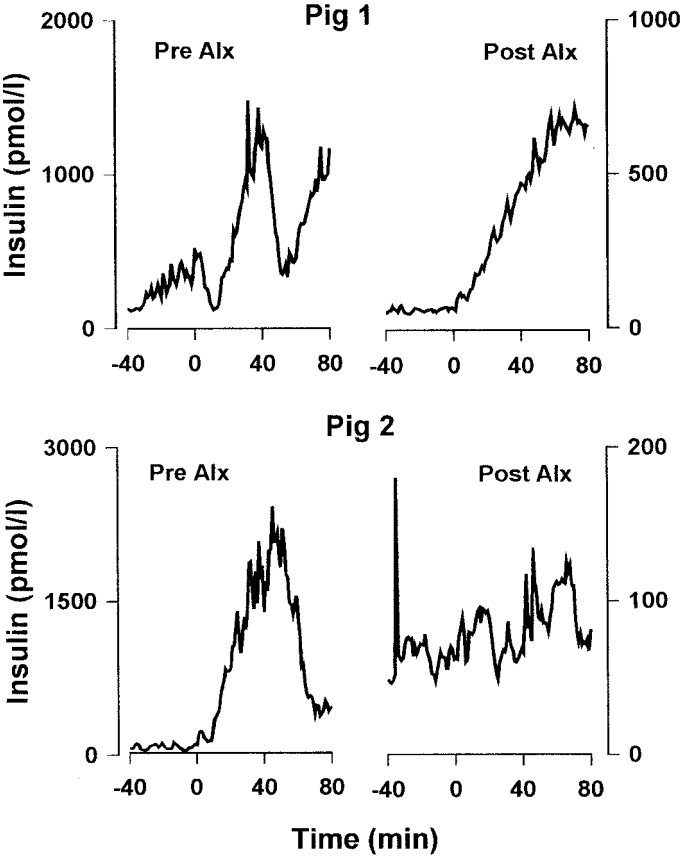

FIG. 4. The insulin concentration profile (measured each minute) from the arterial sampling site in the fasting state (−40 to 0 min) and after ingestion of a mixed meal given at $t = 0$ min in two representative pigs (left, before alloxan administration; right, after alloxan administration). Note the expanded vertical scale after alloxan administration so that pulses can still be seen. The insulin concentration profiles from −40 to 0 min and from 15 to 75 min were deconvolved to determine the pulsatile insulin secretion rate under fasting conditions versus fed conditions, respectively (Fig. 5).

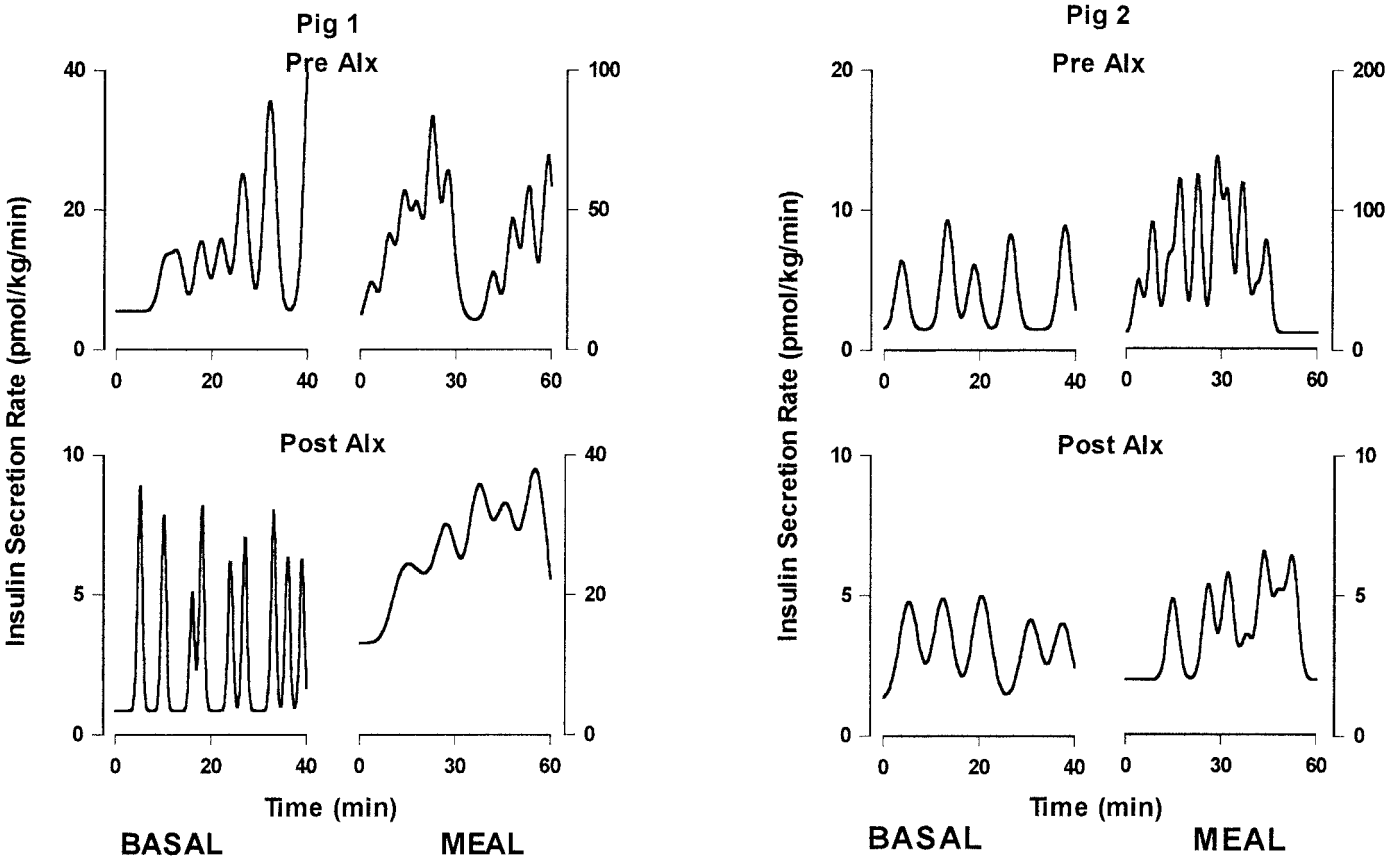

FIG. 5. The insulin secretion rates in two representative pigs (left, pig 1; right, pig 2) in the fasting state (basal) and after meal ingestion before (top) and after (bottom) alloxan administration. Note that the vertical scales are adapted to accommodate the differing data range in each pig and are expanded after alloxan administration so that pulses can be seen.

Total and pulsatile insulin secretion and insulin clearance. Inspection of the individual insulin concentration profiles revealed an increase in the amplitude of insulin pulses after induction of hyperglycemia during the clamp and that this increment was attenuated after alloxan administration (Fig. 11). The clamp-stimulated insulin secretion rate in pigs after alloxan administration was only ~10% of that before alloxan administration during the clamp. Deficient insulin secretion was attributable to a decreased insulin pulse mass (decreased to ~10%) with no change in pulse frequency (Figs. 12 and 13). The pattern of insulin clearance rates was similar to that seen in the meal study (i.e., decreased after alloxan administration) but was not significant during the clamp (one of the five pigs had higher and four had lower insulin clearance rates; Table 2). The relationship between β-cell mass and insulin secretion was comparable to that observed after meal ingestion with a positive correlation between insulin secretion ($r = 0.84$, $P < 0.05$) and insulin pulse mass ($r = 0.82$, $P < 0.05$) but no relationship with insulin pulse interval.

As in the meal study, examination of the insulin concentration data for regular oscillations by CORRCOS revealed significant oscillations in most pigs (four of five) in the basal fasting state but only one of five pigs in the stimulated hyperglycemic clamp state. The oscillation interval was similar before and after alloxan administration in the fasting state (9.9 ± 1.2 vs. 8.9 ± 1.0 min).

First-phase insulin secretion. First-phase insulin secretion in response to the intravenous glucose bolus given at comparable hyperglycemia (end of clamp) was decreased after alloxan administration (1.4 ± 0.6 vs. 11.6 ± 2.2 nmol · l^{-1} · 12 min^{-1}; $P < 0.001$). There was a positive correlation between first-phase insulin secretion and the insulin pulse mass after alloxan administration ($r = 0.63$, $P < 0.01$).

DISCUSSION

In the present study, we sought to address the hypothesis that the defective pulsatile insulin secretion present in

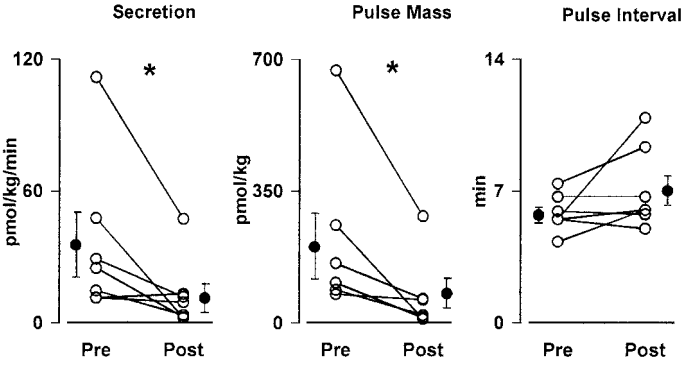

FIG. 6. Mixed meal. The mean insulin secretion rate (left), insulin pulse mass (middle), and interpulse interval (right) are shown for each pig before and after alloxan administration after meal ingestion. The decreased insulin secretion rate after alloxan administration ($P < 0.03$) is due to a decrease in insulin pulse mass ($P < 0.05$) and not any change in pulse frequency (P = NS).

TABLE 2
Pulsatile insulin secretion

	Pulse interval (min/pulse)	Pulse amplitude (pmol/min)	Pulse mass (pmol · kg^{-1} · pulse)	Pulsatile secretion (pmol · kg^{-1} · min)	Total insulin secretion (pmol · kg^{-1} · min)	% Pulsatile insulin secretion	Insulin clearance (l/min)
Meal (n = 7)							
Pre-alloxan							
Fasting	6.5 ± 0.5	10.8 ± 3.4*	24.0 ± 7.1*	4.1 ± 1.5	5.9 ± 2.0	65.1 ± 5.1	0.85 ± 0.1*
Fed	5.8 ± 0.4	77.0 ± 28.2*	203.8 ± 81.7*	35.8 ± 13.5*	42.4 ± 14.1*	80.3 ± 3.7**	1.08 ± 0.14**
Post-alloxan							
Fasting	5.8 ± 0.6	4.5 ± 1.4	12.6 ± 5.4	1.9 ± 0.6	3.2 ± 0.9	54.2 ± 4.0	0.67 ± 0.06
Fed	7.1 ± 0.8	19.7 ± 8.3	75.8 ± 36.0	12.7 ± 6.0	21.3 ± 8.4	54.1 ± 3.2	0.69 ± 0.14
Clamp (n = 5)							
Pre-alloxan							
Fasting	7.3 ± 0.5*	7.7 ± 0.7*	22.4 ± 04.3**	3.1 ± 0.5	4.8 ± 0.6	65.0 ± 6.9	0.89 ± 0.14
Clamp	5.5 ± 0.7	42.6 ± 17.7*	80.9 ± 19.0**	16.0 ± 5.5**	31.1 ± 6.1**	47.1 ± 7.8	0.64 ± 0.17
Post-alloxan							
Fasting	4.7 ± 0.3	4.2 ± 1.4	14.1 ± 6.4	3.1 ± 1.4	4.3 ± 1.4	65.2 ± 6.2	0.62 ± 0.04
Clamp	5.7 ± 0.5	3.4 ± 1.5	8.5 ± 4.3	1.5 ± 0.6	2.8 ± 0.6	45.0 ± 10.6	0.42 ± 0.08

Data are means ± SE. The calculated insulin secretion rate and parameters for pulsatile insulin secretion before and after alloxan administration after glucose injection and during the hyperglycemic clamp. *$P < 0.05$; **$P < 0.01$ before versus after alloxan administration.

patients with type 2 diabetes can be recapitulated by a selective decrease in β-cell mass achieved by alloxan administration in a porcine model. The data reported here support this hypothesis.

Type 2 diabetes in humans is characterized by fasting hyperglycemia with an exaggerated postprandial glycemic excursion, both of which were observed in the present pig model. The insulin concentration in the systemic circulation generally has been reported as comparable in patients with type 2 diabetes and control subjects during fasting (1,5,18) but decreased compared with control subjects early after meal ingestion (1,16,19–21). We previously reported that increased insulin secretion after meal ingestion is achieved by an ~600% amplification of insulin pulse mass (22). Because defective insulin secretion in patients with type 2 diabetes is most evident in the fed state (5) and to examine the effect of a partial decrease in β-cell mass on insulin secretion, we focused on pulsatile insulin release after ingestion of a mixed meal. In the present porcine model, we were able to demonstrate that a partial and selective β-cell deficiency results in decreased insulin secretion in response to meal ingestion that is due to a deficit in the quantity of insulin secreted with each insulin secretory burst while the insulin secretory burst frequency was unchanged. This closely mimics the abnormal pattern of pulsatile insulin release recently observed in patients with type 2 diabetes using the same insulin assay and deconvolution techniques (9). In the current study, we also examined the insulin concentration for regular periodicity. In the fasting state, regular oscillations were detected in the majority of animals with a frequency that was comparable to that observed in previous studies that used rhythm analysis under these fasting conditions (23–25), which is ~30% greater than the pulse interval detected by decon-

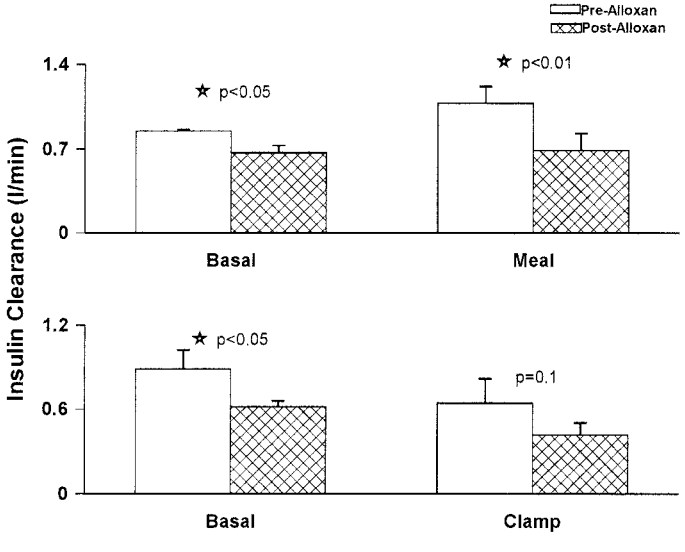

FIG. 7. The clearance rate of endogenously secreted insulin before and after alloxan intervention in the basal state and after a meal or during a clamp. The reduction in β-cell mass induced by alloxan resulted in decreased insulin clearance.

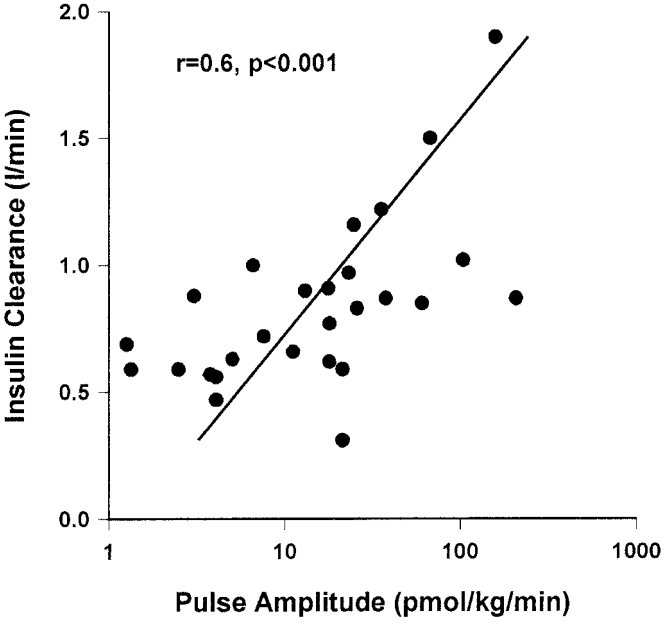

FIG. 8. The relationship between the clearance rate of endogenously secreted insulin and the mean insulin pulse amplitude in each pig before and after meal ingestion and alloxan administration.

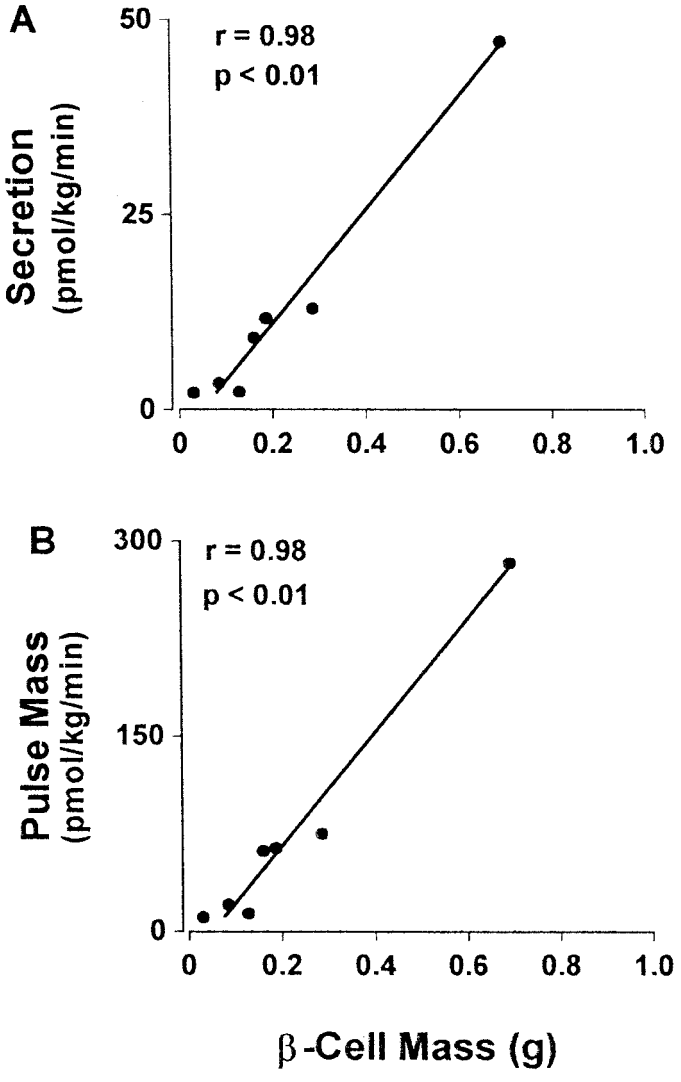

FIG. 9. There was a positive relationship between β-cell mass and both insulin secretion (*A*) and insulin pulse mass (*B*) after meal ingestion in pigs that received alloxan ($n = 7$).

volution, presumably reflecting this degree of irregularity of insulin secretory bursts (deconvolution does not require a constant pulse interval in contrast to spectral analysis). However, we did not observe statistically significant regular oscillations in the majority of pigs after stimulation of insulin secretion by either enteral or intravenous glucose, which suggests greater irregularity of insulin oscillations after glucose stimulation. A primary assumption of spectral analysis methods is that there is stationarity in the data set. However, after glucose stimulation, aggressive nonstationarity is evident in the insulin concentration profiles, so it is not surprising that spectral methods are unable to accommodate these data sets. Some previous studies reported a disturbance of insulin concentration rhythms in patients or in relatives of patients with type 2 diabetes (24,25). However, a recent study that used the same ELISA insulin assay that we used here also did not report any disturbance in pulse rhythm by spectral analysis in patients with type 2 diabetes (26). Therefore, the issue of whether there is a rhythm disturbance (altered regular periodicity) in insulin concentrations in patients with type 2 diabetes remains to be resolved.

In a previous study of partial β-cell deficiency induced by streptozocin in baboons, an abnormal pattern of pulsatile insulin secretion was observed (27). However, the current study differs from that in several ways. First, in the study of baboons, several doses of streptozocin were used and insulin secretion was studied after intravenous glucose and arginine injections. The technique for examining pulses did not quantify pulse mass or the rate of insulin secretion. The mean fasting plasma glucose concentration in the treated baboons increased only from 4.6 to 5.8 mmol/l. Despite these differences, the reported decline of insulin pulse amplitude with no change in pulse frequency observed in the baboons after streptozocin administration is consistent with the decrease in pulse mass (and amplitude) and unchanged pulse frequency evident in the current porcine model. One year after hemipancreatectomy, humans have impaired glucose tolerance (28) and decreased first-phase insulin release (29). However, no information is available concerning pulsatile insulin release in these patients. A 64% pancreatectomy in dogs also led to a decrease in insulin secretion in response to arginine that was most pronounced at increased plasma glucose concentrations (i.e., glucose potentiation was decreased) (30). In humans after hemipancreatectomy and dogs after an approximately two-thirds pancreatectomy, both the fasting plasma glucose and the insulin concentrations (measured by conventional immunoassay) were normal, raising the question, "How does a decreased capacity for insulin

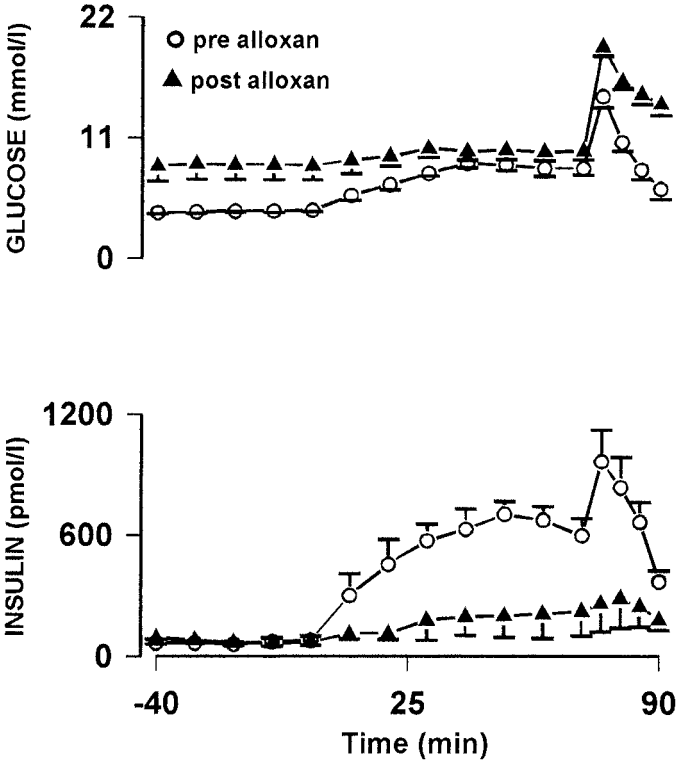

FIG. 10. Mean plasma glucose and arterial insulin concentrations in the fasting state (−40 to 0 min) and during a hyperglycemic clamp (0–70 min) before and after alloxan administration. At $t = 0$ min, the glucose infusion was initiated to achieve a steady-state hyperglycemic clamp at $t = 30$ min. Sampling for measurement of insulin concentrations was performed every minute from −40 to 0 for the basal period and from 30 to 70 min for the clamp period. At $t = 70$ min, an intravenous glucose bolus was given to elicit first-phase insulin secretion (at comparable glucose concentrations in the studies before and after alloxan administration).

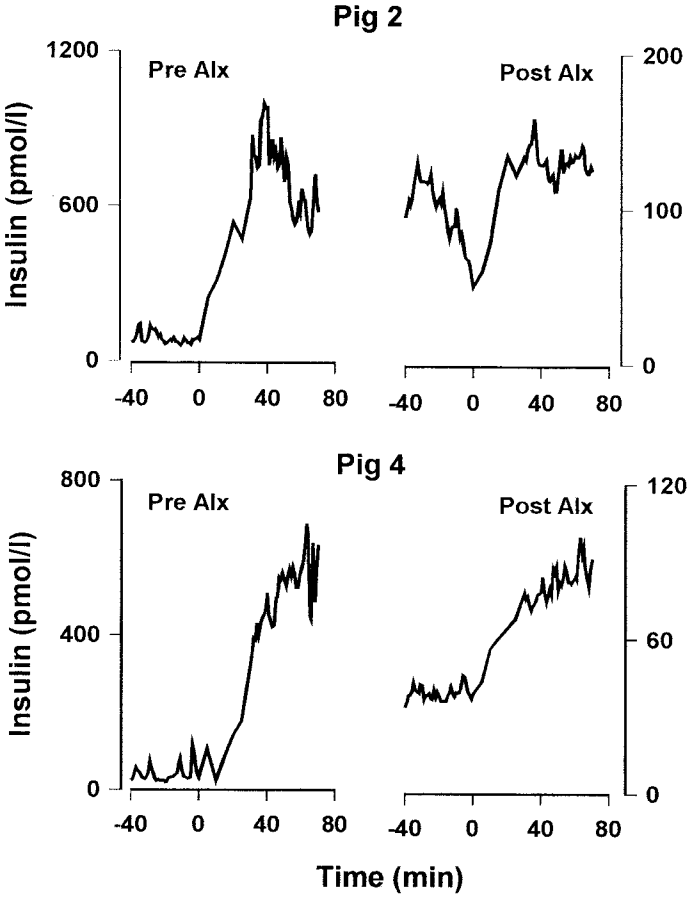

FIG. 11. Individual insulin concentration profiles in representative pigs before and after alloxan administration in the basal fasting state (−40 to 0 min) and during the hyperglycemic clamp (0–70 min). Note the expanded vertical scales after alloxan administration. Insulin concentrations were obtained every minute from –40 to 0 min and from 30 to 70 min for deconvolution of insulin secretion rates (see Fig. 11). Insulin was measured at 5-min intervals from 0 to 30 min during the period when the glucose infusion rate was initiated and increased rapidly to achieve steady-state hyperglycemia by t = 30–70 min.

secretion adapt to prevent the development of diabetes?" The possibilities were examined by Marincola et al. (31) in a study of dogs that had either sham surgery or ~80% pancreatectomy. In these studies, pancreatic insulin output was measured directly by sampling from the portal vein. In the fasting state, insulin output was decreased to ~30% of control values after 80% pancreatectomy, whereas the simultaneous plasma insulin concentration in the systemic circulation was comparable in the pancreatectomy and control animals. These data suggest that hepatic insulin clearance of endogenously secreted insulin was decreased by ~60% in the dogs that underwent partial pancreatectomy.

In the present study, we also observed decreased clearance of endogenously secreted insulin in the setting of a decrease in β-cell mass. This approach is to be contrasted to measuring insulin clearance by infusing exogenous insulin, which has been shown to be unaffected by a partial pancreatectomy (30). We previously showed that partial suppression of insulin secretion achieved with a low-dose infusion of somatostatin reduces the clearance rate of endogenously secreted insulin (32). In that study, the insulin clearance rate was closely correlated to the insulin pulse amplitude. We speculated that the clearance rate of endogenously secreted insulin is related directly to the pulse and amplitude of insulin secretory bursts, so when the pulse amplitude decreases (as a result of decreased β-cell mass or somatostatin), the hepatic extraction of secrete insulin also decreases. We further hypothesized that this dual mechanism for the regulation of insulin delivery to the systemic circulation (modulation of insulin secretion rate with an associated modulation of the insulin clearance rate) serves to buffer the delivery of insulin to the systemic circulation. The present study lends support to these hypotheses. Of note, although the rate of insulin clearance measured in patients with type 2 diabetes has been reported to be unaltered when insulin is infused exogenously (in a nonpulsatile manner into the systemic circulation) (33,34), it is decreased when estimated endogenously (35). Because the defect of insulin secretion in patients with type 2 diabetes is characterized by a decreased pulse mass (9), these data support the notion that in this disease, the seemingly normal or near-normal insulin concentrations in the peripheral circulation may be due in part to a compensatory decrease in the rate of hepatic extraction of insulin as a result of the decreased pulse mass of secreted insulin. The present studies do not address the specific mechanism that accounts for the relationship between pulse amplitude and insulin clearance.

In the current study, we also observed hyperglucagonemia in the pigs that were treated with alloxan. Patients with type 2 diabetes also have abnormalities in glucagon secretion (36). Thus, in the fasting state, despite hyperglycemia, the glucagon concentration is not suppressed and after ingestion of a mixed meal is even higher than that seen in control subjects (37–39). The same pattern is observed in the present porcine model, which suggests that deficient β-cell mass alone and/or chronic hyperglycemia may lead to this defect in α-cell function. These data suggest that hyperglucagonemia in type 2 diabetes may be due to loss of paracrine inhibition of α-cell secretion by intra-islet insulin (40), although this postulate clearly merits further investigation.

From the present model, it is apparent that many of the characteristics of impaired insulin release present in patients with type 2 diabetes can be reproduced by a partial selective loss of β-cells. How are these different aspects of insulin release related, and what is the underlying mechanism? One possible link is the magnitude of the immediately secretable insulin pool. This pool has been recognized for many years as a physiological concept arising from the observed biphasic nature of insulin release in response to an acute glucose challenge (41). Grodsky (42) proposed that the first phase of insulin release was due to the exocytosis of insulin secretory granules docked at the plasma membrane with the later phase of release being related to the movement of undocked granules to the membrane thereafter. It has been possible only recently to visualize directly the granule traffic within secretory cells and to gain insights into the anatomical nature and regulation of the proposed immediately secretable pool. The immediately secretable insulin pool is now confirmed to consist of the insulin vesicles docked at the plasma membrane (43). Recent studies of granule traffic and exocytosis in single cells show that the net rate of movement of vesicles from the remote intracellular vesicle pool to the

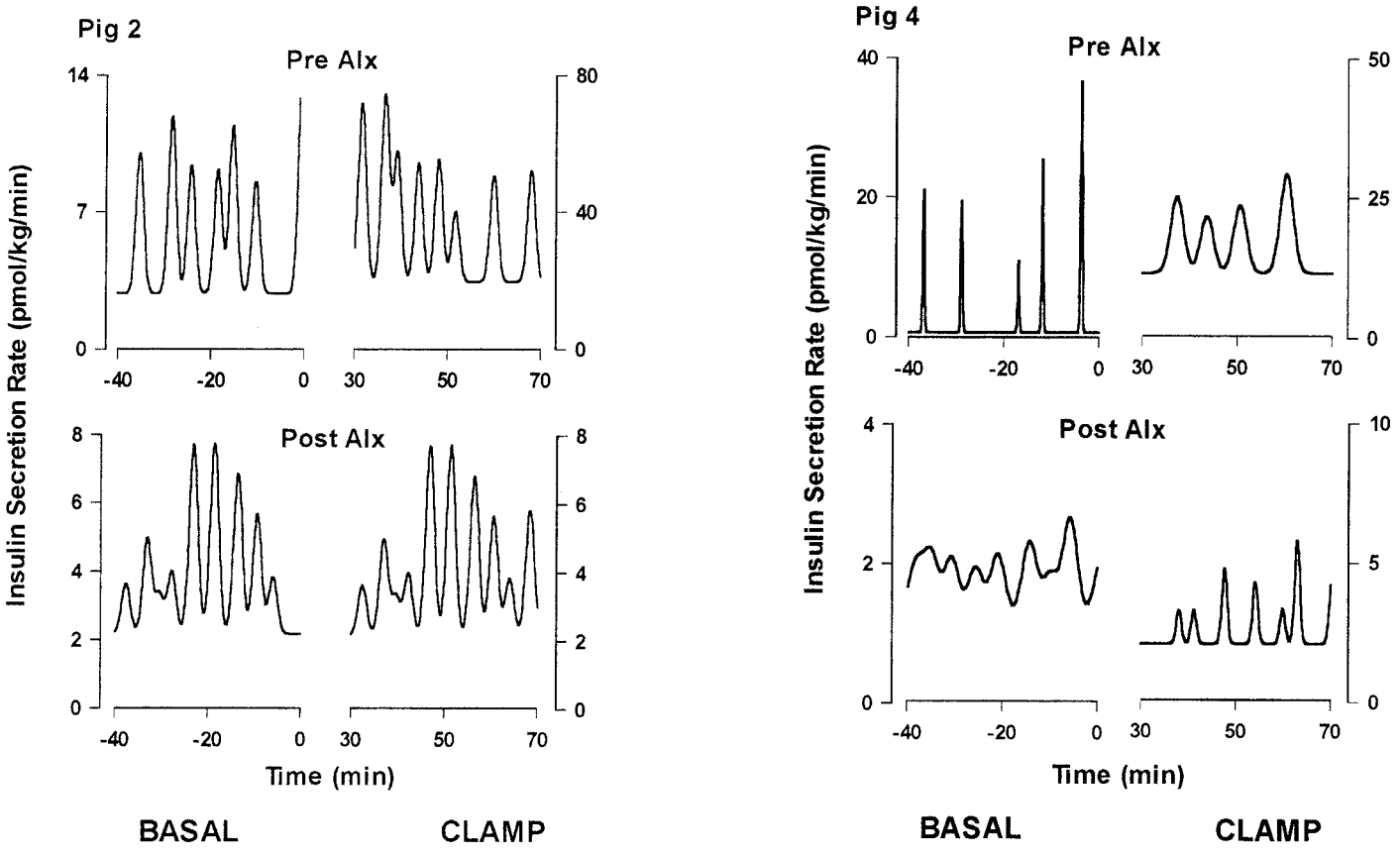

FIG. 12. Secretion profiles in two individual pigs (pig 2, left; pig 4, right) before and after alloxan administration in the fasting (basal) state (−40 to 0 min) and during the clamp (30–70 min). Vertical scales expanded to individual secretion profiles.

membrane-bound pool depends on the relative rate of vesicles being docked onto the membrane versus the rate of their release, in which some membrane-bound vesicles become undocked and return to the intracellular pools (44). In the chromaffin cell, acute stimulation of catecholamine secretion results in a rate of exocytosis that exceeds the maximal capacity of the cell to replete this pool from the remote pool so that the membrane-bound vesi-

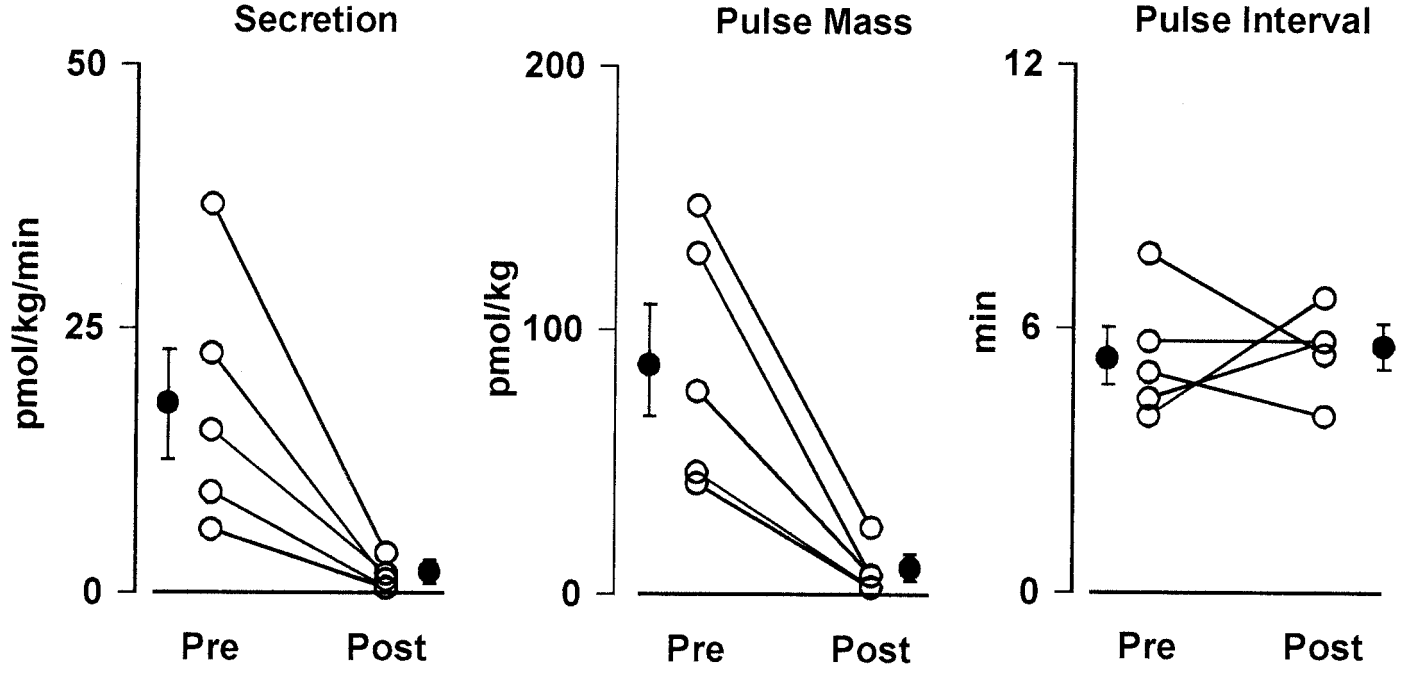

FIG. 13. Clamp. The mean insulin secretion rate (left), pulse mass (middle), and pulse interval (right) for each pig are shown before and after alloxan administration. The decreased insulin secretion rate during the clamp ($P < 0.01$) after alloxan treatment was due to decreased insulin pulse mass ($P < 0.01$) with no change in pulse frequency.

cles are at least transiently depleted (45). If the demand for secretion imposed on a secretory cell continued to exceed the capacity for the forward movement of vesicles from the large remote pool of granules to the cell membrane, then the membrane-bound "first-phase pool" would be depleted. Assuming that insulin release during a spontaneous insulin burst also is derived from the docked insulin secretory granules, one would predict that depletion of this pool would result in a concurrent decrease in both spontaneously pulsatile and first-phase insulin secretion.

Support of the above model is provided by the observation that both pulsatile insulin burst mass and first-phase insulin release were restored at least partially by a period of overnight inhibition of insulin release imposed by a somatostatin infusion in patients with type 2 diabetes (9). Culture of human islets at high glucose concentrations leads to depletion of insulin stores and decreased first-phase insulin release (46). Culture of human islets with high glucose concentrations along with an inhibitor of insulin secretion, diazoxide, results in a relative sparing of insulin stores and enhancement of first-phase insulin release (47) and insulin pulse amplitude (48). If available insulin stores are critical for secretion of insulin secretory bursts of an appropriate size, then chronic high glucose concentration in nondiabetic individuals would be expected to lead to diminished insulin secretion. When plasma glucose was sustained at ~12 mmol/l in nondiabetic healthy humans for 36 h, insulin secretion was decreased and hepatic insulin clearance was increased (49). Because almost all insulin is secreted in insulin pulses, it is safe to infer that the decrease in insulin secretion in that study was characterized by decreased insulin pulses and that this also may have been the cause for the decreased hepatic insulin clearance. In the current study, the decreased number of β-cells present after alloxan administration is required to provide enhanced insulin secretion per cell as well as to be exposed to chronic increased glucose concentrations. The direct relationship between the extent that β-cell mass was reduced by alloxan and the glucose-stimulated insulin secretion rate (after meal or infusion) observed in the present study also is generally supported in this model. It also is possible that some of the alterations of β-cell function observed in the present porcine model are due to sustained injury to surviving β-cells by alloxan administration, although the toxic action of alloxan generally is believed to result in cell death or full recovery. Few data are available on insulin stores in islets from patients with type 2 diabetes, although, generally, these data suggest a loss of total insulin stores (50,51).

In summary, the present study reveals that a partial decrease in β-cell mass results in impaired insulin secretion particularly during enteral or intravenous glucose, which is mechanistically due to a selective decrease in insulin secretory burst mass. Whereas this defect results in a major decline in prehepatic insulin secretion, the effect on delivery of insulin to the systemic circulation is significantly offset by a corresponding fall in hepatic insulin clearance. Insulin secretion and insulin pulse mass were related directly to the β-cell mass. Data from this and previous studies suggest that the decrease in hepatic clearance of endogenously secreted insulin is due to the concurrent decrease in the amplitude of insulin concentration pulses presented to the liver. The specific mechanism to account for the correlation between portal vein insulin concentration amplitude and hepatic insulin clearance remains to be determined.

ACKNOWLEDGMENTS

We acknowledge funding for this project by the Wellcome Trust (project grant) and a Novo Nordisk educational grant. Support for costs of the glucagon assays was made available by the European Association for the Study of Diabetes. L.L.K. was supported by a postdoctoral fellowship from the Danish Medical Research Council.

We acknowledge the excellent technical assistance of Jaqi Armstrong and Joan York (assistance with pig studies and insulin assays); Paula Azimi (with calculations); Christiane Jaminet and Angella Rombaux (glucagon assays); Don Henderson, Duncan McNeil, and Graham Grady for assistance with animal husbandry; and Kim Denkers for editorial assistance.

REFERENCES

1. Perley MJ, Kipnis DM: Plasma insulin responses to oral and intravenous glucose: studies in normal and diabetic subjects. *J Clin Invest* 46:1954–1962, 1967
2. Porte D Jr: β-cells in type 2 diabetes mellitus. *Diabetes* 40:166–180, 1991
3. Seltzer HS, Allen EW, Herron AL Jr, Brennan MT: Insulin secretion in response to glycemic stimulus: relation of delayed initial releases to carbohydrate intolerance in mild diabetes mellitus. *J Clin Invest* 46:323–335, 1967
4. Weir GC: Non-insulin dependent diabetes mellitus: interplay between β-cell inadequacy and insulin resistance. *Am J Med* 73:461–464, 1982
5. Polonsky KS, Given BD, Hirsch LJ, Tillil H, Shapiro ET, Beebe C, Frank BH, Galloway JA, Van Cauter E: Abnormal patterns of insulin secretion in non-insulin-dependent diabetes mellitus. *N Engl J Med* 318:1231–1239, 1988
6. Elahi D: In praise of the hyperglycemic clamp. A method for assessment of beta-cell sensitivity and insulin resistance. *Diabetes Care* 19:278–286, 1996
7. Pørksen N, Munn J, Steers S, Vore S, Veldhuis J, Butler PC: Pulsatile insulin secretion accounts for 70% of total insulin secreted during fasting. *Am J Physiol* 269:E478–E488, 1995
8. Pørksen N, Nyholm B, Veldhuis JD, Butler PC, Schmitz O: In humans at least 75% of insulin secretion arises from punctuated insulin secretory bursts. *Am J Physiol* 273:E908–E914, 1997
9. Laedtke T, Kjems LL, Pørksen N, Schmitz O, Veldhuis JD, Kao PC, Butler PC: Overnight inhibition of insulin secretion restores pulsatility and the proinsulin/insulin ratio in type 2 diabetes. *Am J Physiol* E520–E528, 2000
10. Klöppel G, Löhr M, Habich K, Oberholzer M, Heitz PU: Islet pathology and the pathogenesis of type 1 and type 2 diabetes mellitus revisited. *Surv Synth Pathol Res* 4:110–125, 1985
11. Marshall M: Induction of chronic diabetes by streptozotocin in the miniature pig. *Res Exp Med* 175:187–196, 1979
12. Andersen L, Dinesen B, Jorgensen PN, Poulsen F, Roder ME: Enzyme immunoassay for intact human insulin in serum or plasma. *Clin Chem* 39:578–582, 1993
13. Luyckx AS: Immunoassays for glucagons. In *Glucagon, Molecular Physiology, Clinical and Therapeutic Implications*. Lefèbvre PJ, Unger RH, Eds. Oxford, Pergamon Press, 1972, p. 285–298
14. Song SH, McIntyre SS, Shah H, Veldhuis JD, Hayes P, Butler PC: Direct measurement of pulsatile insulin secretion from the portal vein in human subjects. *J Clin Endocrinol Metab* 85:4491–4499, 2000
15. Veldhuis JD, Johnson ML: Deconvolution analysis of hormone data. *Methods Enzymol* 210:539–575, 1992
16. Harmer SL, Hogenesch JB, Straume M, Chang H-S, Han B, Zhu T, Wang X, Kreps J, Kay SA: Orchestrated transcription of key pathways in Arabidopsis by the circadian clock. *Science* 290:2110–2113, 2000
17. Plautz JD, Straume M, Stanewesky R, Jamison CF, Brandes C, Dowse HB, Hall JC, Kay SA: Quantitative analysis of *Drosophila period* gene transcription in living animals. *J Biol Rhythms* 12:204–217, 1997
18. Pørksen N, Munn S, Steers J, Veldhuis JD, Butler PC: Impact of sampling technique on appraisal of pulsatile insulin secretion by deconvolution and cluster analysis. *Am J Physiol* 269:E1106–E1114, 1995

19. Temple RC, Carrington CA, Luzio SD, Owens DR, Schneider AE, Sobey WJ, Hales CN: Insulin deficiency in non-insulin-dependent diabetes. *Lancet* 1: 293–295, 1989
20. Butler PC, Rizza RA: Contribution to postprandial hyperglycemia and effect on initial splanchnic glucose clearance of hepatic glucose cycling in glucose-intolerant or NIDDM patients. *Diabetes* 40:73–81, 1991
21. Davies MJ, Metcalfe J, Gray IP, Day JL, Hales CN: Insulin deficiency rather than hyperinsulinaemia in newly diagnosed type 2 diabetes mellitus. *Diabet Med* 10:305–312, 1993
22. Pørksen N, Munn S, Steers J, Veldhuis JD, Butler PC: Effects of glucose ingestion versus infusion on pulsatile insulin secretion: the incretin effect is achieved by amplification of insulin secretory burst mass. *Diabetes* 45: 1317–1323, 1996
23. Goodner CJ, Walike BC, Koerker DJ, Ensinck JW, Brown AC, Chideckel EW, Palmer J, Kalnasy L: Insulin, glucagon, and glucose exhibit synchronous, sustained oscillations in fasting monkeys. *Science* 195:177–179, 1977
24. Lang DA, Matthews DR, Peto J, Turner RC: Cyclic oscillation of basal plasma glucose and insulin concentrations in human beings. *N Engl J Med* 301:1023–1027, 1979
25. O'Rahilly S, Turner RC, Matthews DR: Impaired pulsatile secretion of insulin in relatives of patients with non-insulin-dependent diabetes. *N Engl J Med* 318:1225–1230, 1988
26. Ritzel R, Schulte M, Pørksen N, Nauck MS, Holst JJ, Juhl C, März W, Schmitz O, Schmiegel WH, Nuack MA: Glucagon-like peptide 1: increase secretory burst mass of pulsatile insulin secretion in patients with type 2 diabetes and impaired glucose tolerance. *Diabete*s 50:776–784, 2001
27. Goodner CJ, Koerker DJ, Weigle DS, McCulloch DK: Decreased insulin- and glucagon-pulse amplitude accompanying β-cell deficiency induced by streptozocin in baboons. *Diabetes* 38:925–930, 1989
28. Kendall DM, Sutherland DER, Najarian JS, Goetz FC, Robertson RP: Effects of hemipancreatectomy on insulin secretion and glucose tolerance in healthy humans. *N Engl J Med* 322:898–903, 1990
29. Seaquest ER, Robertson RP: Effects of hemipancreatectomy on pancreatic alpha and beta cell function in healthy human donors. *J Clin Invest* 89:1761–1766, 1992
30. Ward WK, Wallum BJ, Beard JC, Toborsky GJ Jr, Porte D Jr: Reduction of glycemic potentiation: sensitive indicator of β-cell loss in partially pancreatectomized dogs. *Diabetes* 37:723–729, 1988
31. Marincola F, Cobb LF, Horaguchi A, Maeda M, Merrell R: Accommodation to a reduced islet cell mass in dogs. *Am J Physiol* 247:E456–E461, 1984
32. Pørksen N, Munn SR, Steers JL, Veldhuis JD, Butler PC: Effects of somatostatin on pulsatile insulin secretion: selective inhibition of insulin burst mass. *Am J Physiol* 270:E1043–E1049, 1996
33. DeFronzo RA, Simonson D, Ferrannini E: Hepatic and peripheral insulin resistance: a common feature of type 2 (noninsulin-dependent) and type 1 (insulin-dependent) diabetes mellitus. *Diabetologia* 23:313–319, 1982
34. Firth R, Bell P, Rizza R: Insulin action in non-insulin-dependent diabetes mellitus: the relationship between hepatic and extra hepatic insulin resistance and obesity. *Metabolism* 36:1091–1095, 1987
35. Sando H, Lee YS, Iwamato Y, Ikeuchi M, Kosaka K: Isoproterenol-stimulated C-peptide and insulin secretion in diabetic and nonobese normal subjects: decreased hepatic extraction of endogenous insulin in diabetics. *J Clin Endocrinol Metab* 51:1143–1149, 1980
36. Lefèbvre PJ: Glucagon and diabetes. In Glucagon III. *Handbook of Experimental Pharmacology*, Vol. 123. Lefèbvre P, Ed. Berlin, Springer-Verlag, 1996, p. 115–131
37. Sherwin RS, Fisher M, Hendler R, Felig P: Hyperglucagonemia and blood glucose regulation in normal, obese and diabetic subjects. *N Engl J Med* 294:455–461, 1976
38. Raskin P, Unger RH: Hyperglucagonemia and its suppression: importance in the metabolic control of diabetes. *N Engl J Med* 299:433–436, 1978
39. Reaven GM, Chen Y-DI, Swislocki ALM, Jaspan JP: Documentation of hyperglucagonemia throughout the day in nonobese and obese patients with non-insulin dependent diabetes mellitus. *J Clin Endocrinol Metab* 64: 106–110, 1987
40. Paolisso G, Sgambato S, Passariello N, Varricchio M, Scheen A, D'Onofrio F, Lefèbvre PJ: Pulsatile insulin delivery is more efficient than continuous infusion in modulating islet-cell function in normal subjects and in patients with type 1 diabetes. *J Clin Endocrinol Metab* 66:1120–1126, 1988
41. Porte D Jr, Pupo AA: Insulin responses to glucose: evidence for a two-pool system in man. *J Clin Invest* 48:2309–2319, 1969
42. Grodsky GM: Threshold distribution hypothesis for packet storage of insulin. II. Effect of calcium. *Diabetes* 21 (Suppl. 2):584–593, 1972
43. Daniel S, Noda M, Straub SG, Sharp GWG: Identification of the docked granule pool responsible for the first phase of glucose-stimulated insulin secretion. *Diabetes* 48:1686–1690, 1999
44. Oheim M, Loerke D, Stühmer W, Chow RH: The last few milliseconds in the life of a secretory granule. Docking, dynamics and fusion visualized by total internal reflection fluorescence microscopy (TIRFM). *Eur Biophys J* 27:83–98, 1998
45. Oheim M, Loerke D, Stühmer W, Chow RH: Multiple stimulation-dependent processes regulate the size of the releasable pool of vesicles. *Eur Biophys J* 28:91–101, 1999
46. Eizirik DL, Korbutt GS, Hellerström C: Prolonged exposure of human pancreatic islets to high glucose concentrations in vitro impairs the β-cell function. *J Clin Invest* 90:1263–1268, 1992
47. Marshak S, Leibowitz G, Bertuzzi F, Socci C, Kaiser N, Gross DJ, Cerasi E, Melloul D: Impaired β-cell function induced by chronic exposure of cultured human pancreatic islets to high glucose. *Diabetes* 48:1230–1236, 1999
48. Song SH, McIntyre SS, Rhodes CJ, Veldhuis JD, Butler PC: Diazoxide attenuates glucose-induced defects in first phase insulin release and pulsatile insulin secretion in human islets. *Diabetes* 49: (Suppl. 1):1771, 2000
49. Boden G, Ruiz J, Cherng-Ju K, Xinhua C: Effects of prolonged glucose infusion on insulin secretion, clearance and action in normal subjects. *Am J Physiol* 270:E251–E258, 1996
50. Wrenshall GA, Bogoch A, Ritchie RC: Extractable insulin of pancreas. Correlation with pathological and clinical findings in diabetic and non-diabetic cases. *Diabetes* 1:87–107, 1952
51. Tasaka Y, Marumo K, Inoue Y, Hirata Y: C-peptide immunoreactivity and insulin content in the diabetic human pancreas and the relation to the stability of diabetic serum glucose level. *Acta Endocrinol* 113:355–362, 1986